

Optimisation of variables for studying dilepton transverse momentum distributions at hadron colliders

A. Banfi^{1,2}, S. Redford³, M. Vesterinen³, P. Waller³, and T. R. Wyatt.³

¹ Institute for Theoretical Physics, ETH Zurich, 8093 Zurich, Switzerland.

² Particle Physics Group, School of Physics and Astronomy, University of Manchester, UK.

Received: 8/9/2010

Abstract. In future measurements of the dilepton (Z/γ^*) transverse momentum, Q_T , at both the Tevatron and LHC, the achievable bin widths and the ultimate precision of the measurements will be limited by experimental resolution rather than by the available event statistics. In a recent paper the variable a_T , which corresponds to the component of Q_T that is transverse to the dilepton thrust axis, has been studied in this regard. In the region, $Q_T < 30$ GeV, a_T has been shown to be less susceptible to experimental resolution and efficiency effects than the Q_T . Extending over all Q_T , we now demonstrate that dividing a_T (or Q_T) by the measured dilepton invariant mass further improves the resolution. In addition, we propose a new variable, ϕ_η^* , that is determined exclusively from the measured lepton directions; this is even more precisely determined experimentally than the above variables and is similarly sensitive to the Q_T . The greater precision achievable using such variables will enable more stringent tests of QCD and tighter constraints on Monte Carlo event generator tunes.

PACS. 12.38.Qk – 13.85.Qk – 14.70.Hp

1 Introduction

The production of $Z/\gamma^* \rightarrow e^+e^-$ and $Z/\gamma^* \rightarrow \mu^+\mu^-$ at hadron colliders provides an ideal testing ground for the predictions of QCD, due to the colourless and relatively background free final state. The dilepton transverse momentum, Q_T , distribution probes QCD radiation in the initial state. At high values of Q_T ($Q_T > 30$ GeV, say), the fixed order perturbative calculations now available at NNLO [1,2] are expected to yield accurate predictions. At low Q_T , soft gluon resummation techniques are required [3], with additional non-perturbative form factors determined in global fits to experimental data such as in [4]. Various event generators are also available [5,6,7,8], matching tree level matrix elements to parton showers tuned to data. Validation and tuning (form factors and parton showers) of these models require comparison with experimental data that have been corrected for detector resolution and efficiency effects. Improved understanding of these production models will increase sensitivity to new physics signals at hadron colliders.

The Q_T distribution has been measured at the Fermilab Tevatron, by the CDF [9] and DØ [10,11,12] Collaborations. The most recent of the above measurements [11,12] used approximately 1 fb^{-1} of data. Although this represents only about one tenth of the anticipated final Tevatron data set, the precision of these measurements was already limited by experimental systematic uncertainties

in the corrections for event selection efficiencies and unfolding of lepton momentum resolution. In order to unfold measured distributions for experimental resolution it is important that the chosen bin widths are not too small compared to the experimental resolution. In the low Q_T region in [11,12], the minimum bin sizes were determined by experimental resolution rather than the available data statistics. The final Tevatron data set will be an order of magnitude larger than that analysed in [11,12]. New ideas are therefore needed in order to exploit fully the data for studying the physics of boson Q_T .

The a_T variable was introduced in [13] and was proposed as a novel variable for studying the Q_T in [14]. Figure 1 illustrates this and other relevant variables defined below. Events with $\Delta\phi > \pi/2$, where $\Delta\phi$ is the azimuthal opening angle of the lepton pair, correspond to approximately 99% of the total cross section. For such events the Q_T is split into two components with respect to an event axis defined as, $\hat{\mathbf{t}} = (\mathbf{p}_T^{(1)} - \mathbf{p}_T^{(2)}) / |\mathbf{p}_T^{(1)} - \mathbf{p}_T^{(2)}|$, where $\mathbf{p}_T^{(1)}$ and $\mathbf{p}_T^{(2)}$ are the lepton momentum vectors in the plane transverse to the beam direction. The component transverse to the event axis is denoted by a_T and the aligned component is denoted by a_L . For events with $\Delta\phi < \pi/2$ this decomposition is not useful and a_T and a_L are defined as being equal to Q_T . a_T is less susceptible than Q_T to the lepton p_T resolution. In addition, the efficiencies of selection cuts on lepton isolation and p_T are

shown in [14] to be less correlated with a_T than Q_T . For studying the low Q_T (non-perturbative) region, a_T is thus a more powerful variable than Q_T . The a_T distribution has subsequently been calculated to NLL accuracy using soft gluon resummation techniques [15].

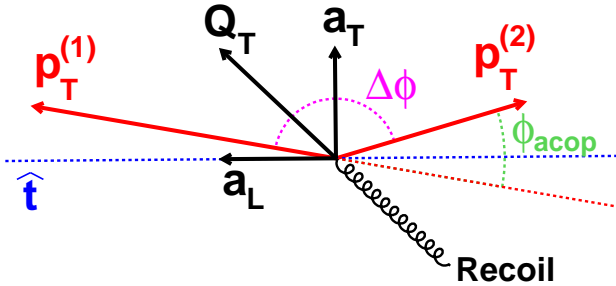


Fig. 1. Graphical illustration in the plane transverse to the beam direction of the variables defined in the text and used to analyse dilepton transverse momentum distributions in hadron colliders.

A recent paper [16] has discussed the idea of using $\Delta\phi$, as an analysing variable that is sensitive to the physics of Q_T , and insensitive to lepton momentum uncertainties¹. Whilst $\Delta\phi$ is primarily sensitive to the same component of Q_T as a_T , the translation from a_T to $\Delta\phi$ depends on the scattering angle θ^* of the leptons relative to the beam direction in the dilepton rest frame. Thus, $\Delta\phi$ is less directly related to Q_T than a_T . As a result, $\Delta\phi$ has somewhat smaller statistical sensitivity to the underlying physics than a_T .

In this paper, we discuss two further ideas to improve experimental precision, whilst maintaining (Q_T) physics sensitivity:

- Dividing a_T , and Q_T by the dilepton invariant mass, Q , thus further reducing the effects of lepton p_T resolution, and almost totally cancelling lepton p_T scale calibration uncertainties.
- Correcting $\Delta\phi$ on an event-by-event basis for the scattering angle, θ^* , thus improving the sensitivity to Q_T .

An overview of the rest of this paper is as follows. In Sect. 2 we give an approximate analytic motivation for the idea of dividing a_T (and Q_T) by Q in order to produce variables with very substantially improved experimental resolution. In Sect. 3 we discuss the idea of correcting $\Delta\phi$ on an event-by-event basis for the scattering angle, θ^* , thus improving the sensitivity to Q_T . In addition, we propose a new variable, $\cos(\theta_n^*)$, which provides a measure of the scattering angle that is based entirely on the measured track directions and is thus extremely well measured experimentally. In Sect. 4 we describe the simple parameterised detector simulation we employ in our MC stud-

¹ We note that the expected distribution of $\Delta\phi$ does have a small residual sensitivity to the lepton p_T measurement. This arises from the cut on Q in the event sample selection, which is affected by the lepton p_T scale and resolution.

ies. In Sect. 5–9 we present the results of our MC studies of the performance of the various candidate variables in terms of their experimental resolution and their sensitivity to the underlying physics. In Sect. 10 we present some conclusions, including our recommendations for the best variables to use in experimental studies of the transverse momentum of dilepton pairs produced at hadron colliders.

2 Mass ratios of a_T and Q_T

For $\Delta\phi \approx \pi$, a_T is given by the approximate formula

$$a_T = 2 \frac{p_T^{(1)} p_T^{(2)}}{p_T^{(1)} + p_T^{(2)}} \sin \Delta\phi$$

and thus the fractional change in a_T with respect to a variation in, say, $p_T^{(1)}$ is given by

$$\frac{\Delta a_T}{a_T} = \frac{p_T^{(2)}}{p_T^{(1)} + p_T^{(2)}} \frac{\Delta p_T^{(1)}}{p_T^{(1)}}$$

The dilepton invariant mass is given by

$$Q = \sqrt{2p^{(1)}p^{(2)}(1 - \cos \Delta\theta)},$$

where $p^{(1)}$ and $p^{(2)}$ are the lepton momenta and $\Delta\theta$ is the angle between the two leptons. Thus, the fractional change in mass with respect to a variation in $p^{(1)}$ is given by

$$\frac{\Delta Q}{Q} = \frac{1}{2} \frac{\Delta p^{(1)}}{p^{(1)}}$$

Since track angles are extremely well measured it can be taken to a very good approximation that

$$\frac{\Delta p_T^{(1)}}{p_T^{(1)}} = \frac{\Delta p^{(1)}}{p^{(1)}}$$

The fractional change in a_T/Q with respect to a variation in $p^{(1)}$ is thus given by

$$\frac{\Delta(a_T/Q)}{(a_T/Q)} = \frac{\Delta a_T}{a_T} - \frac{\Delta Q}{Q} = \left(\frac{p_T^{(2)}}{p_T^{(1)} + p_T^{(2)}} - \frac{1}{2} \right) \frac{\Delta p_T^{(1)}}{p_T^{(1)}}$$

Thus the variations with $p_T^{(1)}$ in a_T and Q partially cancel in the ratio, rendering a_T/Q less susceptible to the effects of lepton p_T resolution than a_T . In particular, in the region of low Q_T then $p_T^{(1)} \approx p_T^{(2)}$ and thus $\Delta(a_T/Q) \approx 0$. Similarly, the quantity Q_T/Q is less susceptible to the effects of lepton p_T resolution than Q_T .

A simple example of an uncertainty in the lepton p_T scale calibration is to consider the p_T of all leptons to be multiplied by a constant factor. It can be seen trivially that in this case a_T , Q_T and Q are all multiplied by the same factor and that the measured a_T/Q and Q_T/Q are unaffected by such a scale uncertainty.

3 Correcting $\Delta\phi$ for the scattering angle

The azimuthal opening angle between the two leptons, $\Delta\phi$, is primarily sensitive to the same component of Q_T as a_T , and is based only on the well measured lepton angles. However, at fixed a_T/Q , $\Delta\phi$ depends on the scattering angle θ^* of the leptons relative to the beam direction in the dilepton rest frame. For convenience, we define the acoplanarity angle, ϕ_{acop} , as $\phi_{\text{acop}} = \pi - \Delta\phi$. For $p_T^{(1)} \approx p_T^{(2)}$ it can be fairly easily shown that

$$a_T/Q \approx \tan(\phi_{\text{acop}}/2) \sin(\theta^*).$$

This suggests that the variable

$$\phi^* \equiv \tan(\phi_{\text{acop}}/2) \sin(\theta^*)$$

may be an appropriate alternative quantity with which to study Q_T .

In the analysis of hadron-hadron collisions, θ^* is commonly evaluated in the Collins Soper frame [17]. However, θ_{CS}^* requires knowledge of the lepton momenta and is thus susceptible to the effects of lepton momentum resolution. Motivated by the desire to obtain a measure of the scattering angle that is based entirely on the measured track directions (since this will give the best experimental resolution) we propose here an alternative definition of θ^* . We apply a Lorentz boost along the beam direction such that the two leptons are back-to-back in the r - θ plane. This Lorentz boost corresponds to $\beta = \tanh\left(\frac{\eta^- + \eta^+}{2}\right)$ and yields the result²

$$\cos(\theta_\eta^*) = \tanh\left(\frac{\eta^- - \eta^+}{2}\right),$$

where η^- and η^+ are the pseudorapidities of the negatively and positively charge lepton, respectively.

We consider two candidate variables

$$\phi_{\text{CS}}^* \equiv \tan(\phi_{\text{acop}}/2) \sin(\theta_{\text{CS}}^*)$$

$$\phi_\eta^* \equiv \tan(\phi_{\text{acop}}/2) \sin(\theta_\eta^*)$$

for further evaluation in terms of their experimental resolution and physics sensitivity.

4 Simple parameterised detector simulation

Monte Carlo events are generated using PYTHIA [18], for the process $p\bar{p} \rightarrow Z/\gamma^*$, in the e^+e^- and $\mu^+\mu^-$ decay channels, and re-weighted in dilepton Q_T and rapidity, y , to match the higher order predictions of RESBOS [19] as in [14]. Electrons and muons are defined at ‘‘particle level’’ according to the prescription in [20], and at ‘‘detector level’’ by applying simple Gaussian smearing to

² The lepton pseudorapidity, η , is defined as $\eta = -\ln[\tan(\frac{\theta}{2})]$, where θ is the polar angle with respect to the beam direction, in the laboratory frame.

the particle level momenta: $\delta(1/p_T) = 3 \times 10^{-3}$ (1/GeV) for muons, which are measured in the tracking detectors; $\delta p/p = 0.4(p/p_0)^{-1/2}$ with $p_0 = 1$ GeV for electrons, which are measured in the calorimeter. In addition, the particle angles are smeared, assuming Gaussian resolutions of 0.3×10^{-3} rad for ϕ and 1.4×10^{-3} for η . These energy, momentum, and angular resolutions roughly correspond to those in the DØ detector [21].

Events are accepted for further analysis if: $70 < Q < 110$ GeV and both leptons satisfy the requirements $p_T > 15$ GeV and $|\eta| < 2$. These selection cuts are made at particle level, unless otherwise stated.

5 Scaling factors

In the following sections, we compare the experimental resolution and physics sensitivity of the various candidate variables. In particular, we compare the variation of the resolution for each variable as a function of that variable. This comparison is facilitated by ensuring that all distributions have approximately the same scale and shape. Compared to Q_T or Q_T/Q , all other variables are on average a factor $\sqrt{2}$ smaller (since a_T and a_L measure one component of Q_T). A simple multiplication by M_Z ($= 91.19$ GeV [22]) corrects for the average Q^{-1} factor in the mass ratio and angular variables and conveniently ensures that all variables have the same units (GeV). Finally, the mean value of $\sin(\theta^*)$ is around ~ 0.85 , and $\tan(\phi_{\text{acop}}/2)$ is scaled by this additional factor. The above factors are summarised in Table 1.

variable	scaling factor
Q_T	1
Q_T/Q	M_Z
a_T	$\sqrt{2}$
a_T/Q	$\sqrt{2}M_Z$
a_L	$\sqrt{2}$
a_L/Q	$\sqrt{2}M_Z$
$\tan(\phi_{\text{acop}}/2)$	$0.85\sqrt{2}M_Z$
ϕ_{CS}^*	$\sqrt{2}M_Z$
ϕ_η^*	$\sqrt{2}M_Z$

Table 1. Scaling factors for different candidate variables.

6 Experimental resolution for dilepton scattering angle

Figure 2 shows the experimental resolution of $\cos(\theta_{\text{CS}}^*)$ and $\cos(\theta_\eta^*)$ in our simulation of dimuon events. The upper row of Figure 2 shows events that satisfy $70 < Q < 110$ GeV; it demonstrates that $\cos(\theta_\eta^*)$ is significantly better measured experimentally than $\cos(\theta_{\text{CS}}^*)$. This is because $\cos(\theta_\eta^*)$ is evaluated using only angular measurements, which are

more precise than the momentum measurements included in the determination of $\cos(\theta_{CS}^*)$.

The variable $\cos(\theta_\eta^*)$ is used in the definition of $\phi_\eta^* = \tan(\phi_{acop}/2) \sin(\theta_\eta^*)$ in Section 3 above. As an aside, we note in addition that a precise determination of the dilepton centre of mass scattering angle that is free from the effects of lepton momentum resolution can also find application in the determination of the forward-backward charge asymmetry of dilepton production at hadron colliders. The experimental resolution in $\cos(\theta_{CS}^*)$ becomes particularly significant in the dimuon channel for very high values of Q for which the lepton momentum resolution is poorest. This is illustrated in the lower row of Figure 2, which shows the experimental resolution of $\cos(\theta_{CS}^*)$ and $\cos(\theta_\eta^*)$ in events that satisfy $500 < Q < 600$ GeV. The advantage of using $\cos(\theta_\eta^*)$ for high mass events is even larger than was the case for $70 < Q < 110$ GeV.

7 Experimental resolution for variables related to dilepton Q_T

Figure 3 compares separately for our dimuon and dielectron simulations, the mean resolution, $|\delta x|$, of various candidate variables, x , as a function of (particle level) x . All variables are scaled by the factors in Table 1.

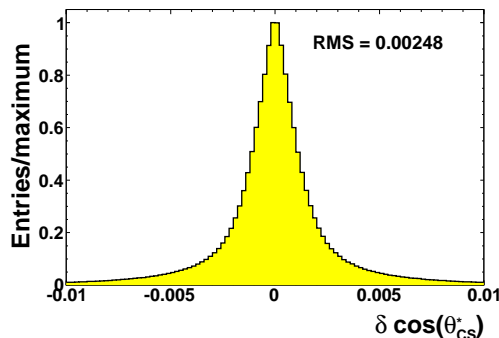
The following observations are made:

- a_T/Q is significantly better measured than a_T , over the entire range.
- Similarly, Q_T/Q is significantly better measured than Q_T .
- Over the full range, a_T and a_T/Q perform better than Q_T and Q_T/Q respectively.
- Compared to a_T/Q , ϕ_{CS}^* has significantly better resolution, and ϕ_η^* better still.
- The most precisely measured variable is $\tan(\phi_{acop}/2)$, since it is determined only from the azimuthal angles of the leptons, whereas the uncertainty on ϕ_η^* includes also the uncertainties on the measured lepton pseudorapidities.

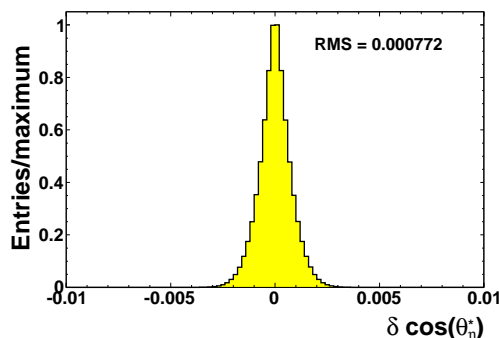
Since the discussion in Section 2 is only approximate, we have investigated empirically various other possible scalings of a_T with Q (with the appropriate scale factor applied, as above). These are illustrated in Figure 4. As expected, it can be seen that when compared to the other variables considered in Figure 4, a_T/Q has the best experimental resolution for all Q_T and irrespective of whether (a) tracker-like or (b) calorimeter-like resolution in the lepton momenta is simulated.

8 Event selection efficiency

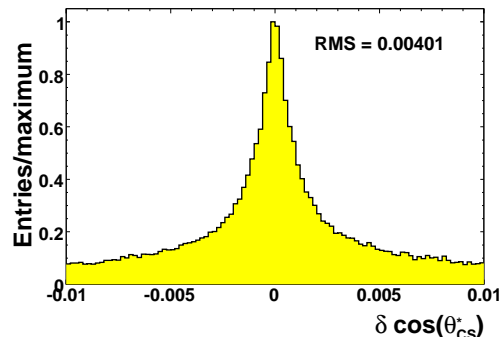
As discussed in [14], the efficiencies of selection cuts on lepton isolation and p_T (for $a_T < p_T^{\text{cut}}$) are less correlated with a_T than Q_T . We have verified that the correlations of these selection efficiencies with a_T/Q and Q_T/Q are essentially identical to those with a_T and Q_T respectively.



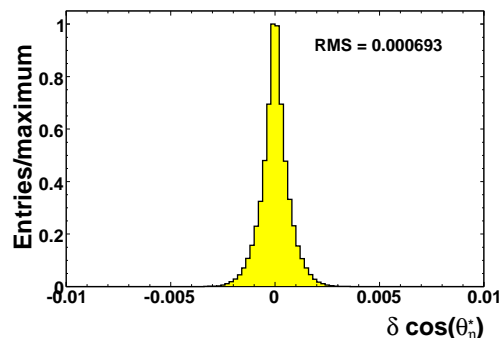
(a) $70 < Q < 110$ GeV



(b) $70 < Q < 110$ GeV

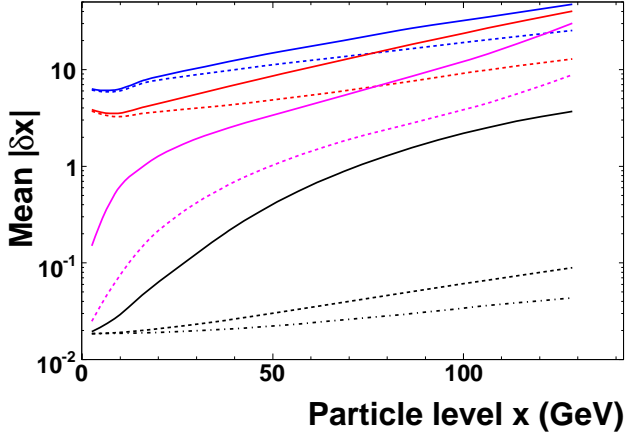


(c) $500 < Q < 600$ GeV

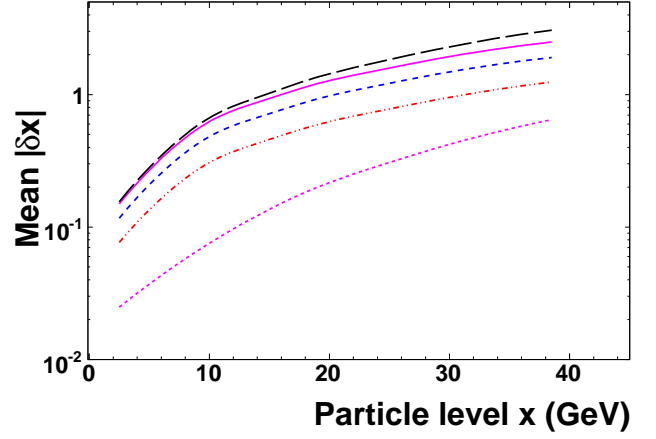


(d) $500 < Q < 600$ GeV

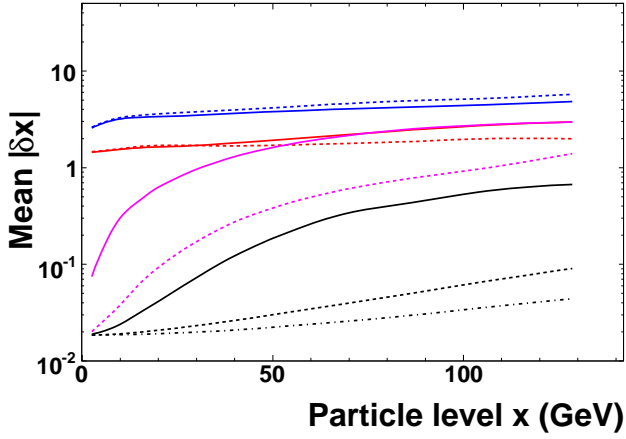
Fig. 2. Distributions of experimental resolutions the dilepton centre of mass scattering angle for events satisfying $70 < Q < 110$ GeV (upper row) and $500 < Q < 600$ GeV (lower row). Figures (a) and (c) show $\cos(\theta_{CS}^*)$. Figures (b) and (d) show $\cos(\theta_\eta^*)$.



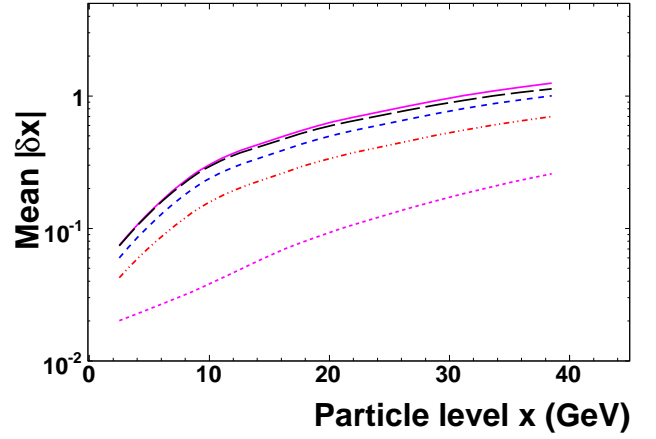
(a) Tracker



(a) Tracker



(b) Calorimeter



(b) Calorimeter

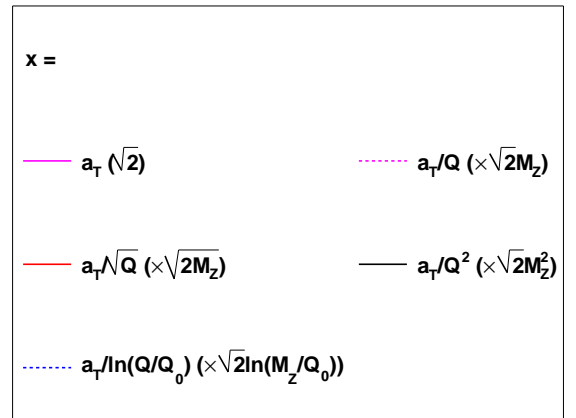
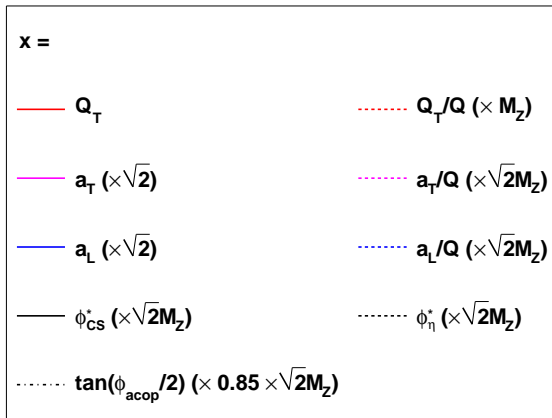


Fig. 3. The mean resolution of each candidate variable, as a function of that variable (scaled by the factors described in the text). Results are presented both for (a) tracker-like and (b) calorimeter-like resolution in the lepton momenta.

Fig. 4. The mean resolution of the variables a_T , a_T/Q , $a_T/Q^{1/2}$, $a_T/\ln(Q/Q_0)$, and a_T/Q^2 , as a function of that variable (scaled by the factors described in the text). Results are presented both for (a) tracker-like and (b) calorimeter-like resolution in the lepton momenta.

$\Delta\phi$ is primarily sensitive to the a_T component of the Q_T . The variables, ϕ_η^* , and ϕ_{CS}^* , are verified to exhibit the same benefits as a_T compared to Q_T , in terms of efficiency dependence.

9 Sensitivity to the physics

Figure 5 shows the particle level, normalised distributions of a_T , $M_Z a_T/Q$ and $\ln(M_Z/Q_0)a_T/\ln(Q/Q_0)$ (with $Q_0 = 1$ GeV) for three ranges of Q . We see that a_T has a mild dependence on Q , while dividing by Q over corrects this dependence. In this respect, we observe that the distribution in $a_T/\ln(Q/Q_0)$ has a smallest dependence on Q , as might be expected from [3].

Experimental measurements of Z boson production are typically made over a fairly wide bin in Q (e.g., 70–110 GeV). One potential concern with measurements of a_T/Q and Q_T/Q is that the increased correlation with Q demonstrated in Figure 5 might degrade the sensitivity to the underlying physics. Since ϕ_η^* behaves approximately as $\phi_\eta^* \approx a_T/Q$, a similar degradation in the physics sensitivity of ϕ_η^* may similarly be expected. In this respect, $a_T/\ln(Q/Q_0)$ is a more suitable variable than a_T/Q for studying the boson Q_T distribution over a wide range in Q . However it has poorer experimental resolution, as was demonstrated in Figure 4.

Using a similar procedure to that described in [14], we study the sensitivity to the underlying physics of the different candidate variables. We run pseudo-experiments to fit for the value of the parameter g_2 , which determines the width of the low Q_T region in RESBOS. Events must meet the requirements described in Section 4, except that these are applied at detector level rather than particle level. Of these events, 1M are assigned as pseudo-data and the remaining events are used to build g_2 templates. All variables are scaled by the factors listed in Table 1, such that the same binning (30 equal width bins in the range 0–30 GeV) can be used. A minimum χ^2 fit determines the statistical sensitivity of each variable to the value of g_2 .

Whilst in [14] we were mostly interested in the low Q_T region, the ideas proposed in this paper also improve experimental resolution at higher Q_T (see Section 7). Thus it is of interest to study the physics sensitivity also in this region. We similarly fit for a parameter K_{Q_T} , which weights events with (particle level) $Q_T > 25$ GeV, by $K_{Q_T}(Q_T - 25)$, and approximately represents the differences between predictions at NLO and NNLO discussed in [11]. Again, after applying the appropriate scaling factors from Table 1, the same binning can be used for each variable³.

The results of the fits to g_2 and K_{Q_T} are presented in Tables 2 and 3 respectively. Results are given separately for particle-level (dimuon) and detector-level (tracker and calorimeter). For both a_T/Q and Q_T/Q , the statistical

³ The first bin is of width 5 GeV (with lower edge at zero) and each consecutive bin is 2 GeV wider than the last. Ten such bins give an upper edge of the last bin at 140 GeV and the fit includes the overflow bin from 140 GeV to ∞ .

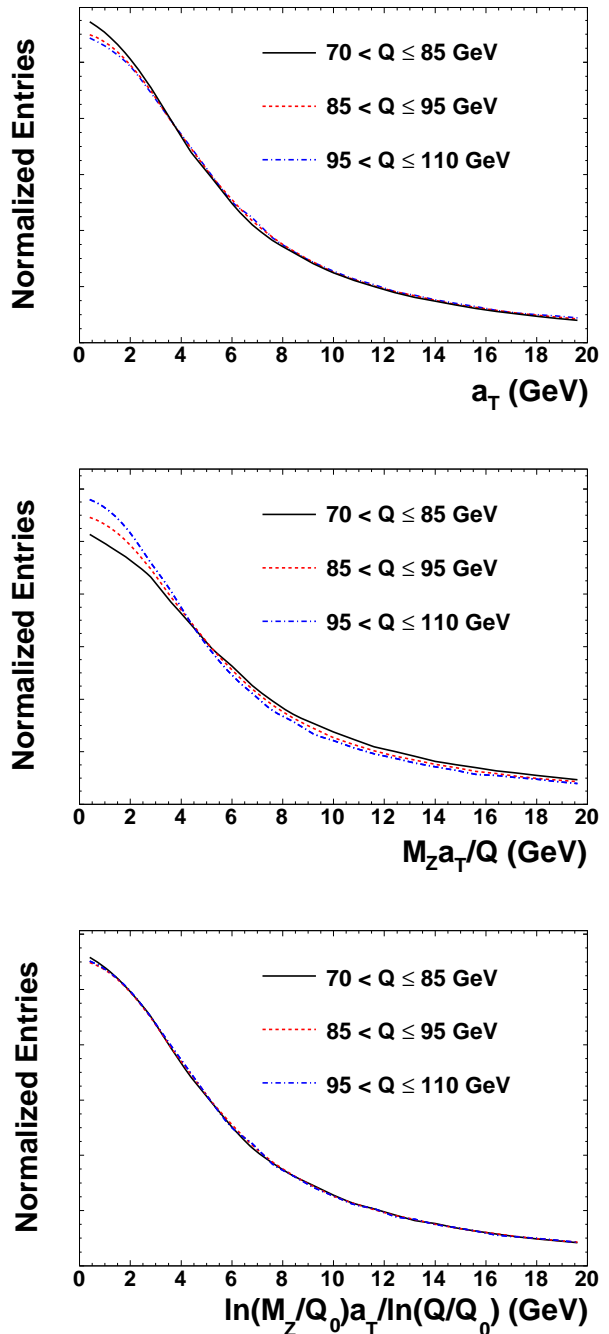


Fig. 5. Comparison of particle level distributions of a_T , $M_Z a_T/Q$ and $\ln(M_Z/Q_0)a_T/\ln(Q/Q_0)$ for three ranges of Q .

sensitivities are essentially the same as those for a_T and Q_T respectively. Thus the effect of the additional Q dependence is shown to be negligible.

The approximately 5% poorer sensitivity of $\tan(\phi_{acop}/2)$, compared to a_T/Q , demonstrates the $\sin(\theta^*)$ ambiguity of the former. The additional factor $\sin(\theta^*)$, present in ϕ_η^* and ϕ_{CS}^* actually recovers the sensitivity to the same level as a_T . In addition, the ϕ_η^* variable, which was shown in

variable	particle level	calorimeter	tracker
Q_T	0.65	0.94	1.41
Q_T/Q	0.65	0.94	1.40
a_T	1.00	1.00	1.00
a_T/Q	1.00	1.01	1.00
a_L	1.21	2.35	4.74
$\tan(\phi_{\text{acop}}/2)$	1.04	1.05	1.04
ϕ_{CS}^*	1.00	1.00	0.99
ϕ_η^*	1.00	1.00	0.99

Table 2. Statistical sensitivity (in %) on the parameter g_2 from fits to the distributions of different of variables. For details see text.

variable	particle level	calorimeter	tracker
Q_T	1.65	1.67	1.82
Q_T/Q	1.66	1.67	1.78
a_T	1.92	1.92	1.96
a_T/Q	1.92	1.92	1.94
a_L	1.98	2.02	2.34
$\tan(\phi_{\text{acop}}/2)$	1.96	1.96	1.98
ϕ_{CS}^*	1.88	1.88	1.90
ϕ_η^*	1.87	1.87	1.92

Table 3. Statistical uncertainty (in %) on the parameter K_{Q_T} (as defined in the text) from fits to the distributions of different of variables. For details see text.

Section 7 to have the best experimental resolution (except for $\tan(\phi_{\text{acop}}/2)$), performs similarly to ϕ_{CS}^* in terms of physics sensitivity.

Of course, the results presented in Tables 2 and 3 represent only the statistical sensitivity of the considered variables when compared to Q_T . As discussed in [14], the systematic uncertainties associated with modelling of detector resolution and efficiency will be significantly smaller using variables that are better measured and less correlated with event selection efficiencies than is the case for Q_T .

10 Summary and conclusions

Measurements of dilepton (Z/γ^*) transverse momentum, Q_T , distributions are crucial for improving models of vector boson production at hadron colliders. The precision of future measurements of the Q_T distribution at the Tevatron and LHC will be totally limited by uncertainties in correcting for detector resolution and efficiency, and the minimum bin sizes will be limited by resolution.

In [14] an alternative variable, a_T , was demonstrated to be significantly less susceptible to such detector effects than Q_T . We have shown in this article that the experimental resolution of a_T can be further improved by taking the ratio to the measured dilepton invariant mass, Q . Similarly, we have demonstrated that the variable Q_T/Q is experimentally more precisely measured than Q_T . No obvious disadvantages of the variable a_T/Q (Q_T/Q) as compared to a_T (Q_T) are found when studying the effi-

ciency dependencies or the physics sensitivity (by making fits to parameters describing the shape of the Q_T distribution).

The acoplanarity angle, ϕ_{acop} , is also sensitive to Q_T . However, it has the approximate dependence $a_T/Q \approx \tan(\phi_{\text{acop}}/2)\sin(\theta^*)$, where θ^* is the scattering angle of the leptons with respect to the beam direction in the dilepton rest frame. Thus ϕ_{acop} is less directly related to Q_T than a_T . We show that correcting $\tan(\phi_{\text{acop}}/2)$ by factor $\sin(\theta^*)$ yields a variable with essentially the same statistical sensitivity as a_T/Q , whilst the experimental resolution is significantly better. Furthermore, using an approximate rest frame determined using only angular information, we propose a new method to measure the scattering angle, θ_η^* , with the best possible experimental resolution. We conclude that in the region of low Q_T the variable $\phi_\eta^* \equiv \tan(\phi_{\text{acop}}/2)\sin(\theta_\eta^*)$ represents the optimal combination of physics sensitivity, experimental resolution and immunity to experimental systematic uncertainties.

For studying the high Q_T region, the optimal variable is Q_T/Q , which is significantly better measured than Q_T , and has no disadvantages in terms of physics sensitivity or efficiency dependence. However, it is interesting to study correlations between the a_T and a_L components of Q_T . Therefore, measurements of ϕ_η^* in the high Q_T region will be complementary to measurements of Q_T/Q .

These further optimisations of variables used to study the Q_T distribution will allow significantly finer binning and smaller unfolding corrections (and thus uncertainties), enabling tighter constraints on vector boson production models.

References

1. K. Melnikov, F. Petriello, Phys. Rev. D **74**, (2006), 114017.
2. S. Catani et al, Phys. Rev. Lett. **103**, (2009), 082001.
3. J. Collins, D. Soper, G. Sterman, Nucl. Phys. B **250**, (1985), 199-224.
4. F. Landry et al, Phys. Rev. D **67**, (2003), 073016.
5. T. Sjöstrand, S. Mrenna, P. Skands, JHEP **05**, (2006), 026.
6. G. Corcella et al, JHEP **0101**, (2001), 010.
7. M. L. Mangano et al, JHEP **0307**, (2003) 001,
8. T. Gleisberg et al, JHEP **0902**, (2009), 007.
9. CDF Collaboration, T. Affolder et al, Phys. Rev. Lett. **84**, (2000), 845.
10. DØ Collaboration, B. Abbott et al, Phys. Rev. D **61**, (2000), 032004; DØ Collaboration, B. Abbott et al, Phys. Rev. L. **84**, (2000), 2792.
11. DØ Collaboration, V. M. Abazov et al, Phys. Rev. Lett. **100**, (2008), 102002.
12. D0 Collaboration, V. M. Abazov et al, arXiv:1006.0618 [hep-ex] submitted to Phys. Lett. B (2010).
13. OPAL collaboration, K. Ackerstaff et al, Eur. Phys. J. C **4** (1998), 47.
14. M. Vesterinen, T. R. Wyatt, Nucl. Instrum. Meth. A **602**, (2009), 432-437.
15. A. Banfi, M. Dasgupta, R. M. Duran Delgado, JHEP **0912**:022 (2009).
16. M. Boonekamp, M. Schott, arXiv:1002.1850v1 [hep-ex] (2010).

17. J. Collins, D. Soper, Phys. Rev. D **16**, (1977), 2219-2225.
18. T. Sjöstrand et al, Comput. Phys. Commun. **135**, (2001), 238.
19. C. Balazs, C.P. Yuan, Phys. Rev. D **56**, (1997), 5558-5583.
20. J. M. Butterworth et al, arXiv:1003.1643v1 [hep-ph] (2010).
21. DØ Collaboration, V. M. Abazov et al, Nucl. Inst. and Meth. A **565**, (2006), 465-537.
22. C. Amsler et al, Phys. Lett. B **667**, (2008), 1.
23. P. Nadolsky et al, Phys. Rev. D **78**, (2008), 013004.